Infrared-laser-induced photodesorption of NH_3 and ND_3 adsorbed on single-crystal Cu(100) and Ag film

Ingo Hussla, H. Seki, T. J. Chuang
IBM Research Laboratory, San Jose, California 95193

Z. W. Gortel,* H. J. Kreuzer, P. Piercy*
Department of Physics, Dalhousie University, Halifax, Nova Scotia, Canada B3H 3J5
(Received 21 January 1985)

Desorption is obtained when ir laser pulses at 3320—3400 cm^{-1} excite the N—H stretching modes of NH_3 and/or ND_3 adsorbed on single-crystal Cu(100) and Ag film surfaces at low temperatures and under ultrahigh-vacuum conditions. While resonant photodesorption occurs with a quantum efficiency of less than 10^{-4} for laser fluence up to 20 mJ/cm^2, no significant isotope selectivity in photodesorption is observed when NH_3 is vibrationally excited in co-adsorbed mixtures of NH_3 and ND_3. Surface coverage, composition, and heat of adsorption of ammonia are determined by conventional thermal desorption, x-ray photoemission, and laser-induced thermal desorption excited by 532-nm light pulses. Molecular desorption is detected by time-of-flight quadrupole mass spectrometry. The desorption behavior is studied as a function of laser frequency and fluence as well as the surface coverage at different substrate temperatures. Calculations of the photodesorption rates based on a master equation including phonon and electronic damping mechanisms are performed. It is shown that the resonant or indirect heating effect caused by the energy damping can explain some but not all of the major experimental observations. The possibility of internal molecular excitation during the desorption process is suggested. This and other dynamic aspects of the ir photodesorption process are also discussed.

I. INTRODUCTION

A laser beam impinging onto an adsorbate-covered surface of a solid can deposit all or part of its energy either (a) into the solid directly, (b) into the surface bond with which an adsorbed molecule is bound to the surface, or (c) into some internal vibrational-rotational mode of the adsorbed molecule. Process (a) can heat up the solid, leading to thermal desorption: we refer to this as direct laser-induced thermal desorption. It is feasible at all laser frequencies at which appreciable absorption of light occurs in the solid.[1—6] In contrast, processes (b) and (c) are resonant in character. The main thrust of this paper is to study photodesorption of NH_3 and ND_3 from Cu(100) by resonant laser-molecular vibrational coupling. Although the desorption phenomenon due to resonant absorption of infrared photons by adsorbed molecules has been observed by Heidberg *et al.*,[7,8] and by Chuang and Seki,[9—12] prior experiments have been rather limited in laser-excitation ranges, and detailed understanding of the basic surface processes involved in the ir photodesorption is still lacking. In this paper the recently obtained experimental data will be analyzed and discussed on the basis of previously developed theories.[13—15] After a brief discussion of the experimental apparatus we present thermal-desorption data for NH_3/Cu(100), which suggest two chemisorption states in a monolayer regime and a physisorbed state in the (2—3)-monolayer regime. Section II C contains the data for photodesorption by resonant layer-molecular vibrational coupling in the frequency range from 3300 to 3450 cm^{-1}. We report on time-of-flight (TOF) measurements and give the frequency and fluence dependence of the ir photodesorption yield[16] (fluence is the time integral of the intensity of a pulsed laser). Section II D presents results from co-adsorbed equal mixtures of NH_3 and ND_3. Section II E then reports an attempt to photodesorb ND_3 from Cu(100) with a low-power laser in the frequency range 2400—2550 cm^{-1}, and the results for NH_3 and ND_3 adsorbed on Ag films are presented in Sec. II F.

Section III is devoted to a thorough analysis of the experimental data using previously developed theories. In Sec. III A we will show that resonant heating[13,14] or indirect heating[11,12] seems to be a very important effect, on the basis of which one can understand the major parts of the data. In Sec. III B we present explicit calculations of photodesorption rates taking only energy transfer via phonons into account.[13] Because the resulting resonant heating is not sufficient, we include in Sec. III C electronic damping in a phenomenological model. In Sec. III D we then analyze the frequency dependence of the photodesorption yield, advancing the idea that in the chemisorbed monolayer only the symmetric stretch vibration of NH_3 is excited, whereas a multilayer random orientation allows in addition the excitation of the antisymmetric stretching mode. In the final section we draw some general conclusions about systems in which, contrary to the NH_3-ND_3/Cu(100) and Ag film systems studied here, one might be able to avoid resonant heating and thus be able to selectively desorb particular isotope species.

II. EXPERIMENTS

A. Apparatus

The apparatus used in the present studies consists of an ultrahigh-vacuum (UHV) chamber equipped with a combination electron spectroscopy for chemical analysis (ESCA) and an Auger-electron spectrometer, an ion gun, a quadrupole mass spectrometer, and a radio-frequency induction heater as described previously.[11,12] A Q-switched Nd:YAG (yttrium-aluminum-garnet) laser (Quanta-Ray) is frequency-doubled to 532 nm and used to pump a dye laser containing Exciton LDS 765 and 867 dyes. The tunable ir pulses in the (2.5—4.2)-μm range are generated in a $LiNbO_3$ crystal from the frequency difference between the 1.064-μm radiation and the dye laser. The pulse duration is 6 nsec and its repetition rate is 10 Hz. The laser linewidth is about 1 cm^{-1} or slightly less. The beam is polarized parallel to the plane of incidence, focused and incident at 75° from the surface normal to cover a surface area of about 5 mm^2. The laser beam enters and leaves the UHV chamber through sapphire windows to minimize scattering of laser light in the vacuum chamber. The visible-light pulses at 532 nm are also used to perform laser-induced thermal-desorption studies.

The mass spectrometer is placed in a line-of-sight arrangement along the surface normal with the ionizer located about 45 mm from the Cu(100) sample. The spectrometer has a time constant of 25 μsec at 10^{-7} and 10^{-8} A, the sensitivity ranges typically used in the experiments. The time-of-flight mass signal is digitized with a Tracor signal averager with 2-μsec time resolution which is triggered by the laser-synchronization pulse. A Cu(100) single crystal is held with a manipulator and can be cleaned by Ar^+ bombardment, annealed by rf heating, and cooled to about 90 K with liquid N_2. Ammonia gas is dosed through a small copper tube directly facing the crystal. The amount of surface coverage is determined from ESCA intensity analyses and from thermal-desorption spectra.

NH_3-ND_3 mixtures are prepared in the manifold just before exposure. Surface concentrations are determined by laser-induced thermal desorption using green (532-nm) laser pulses. For this procedure the masses 17 and 20 are traced following laser heating of the surface and the relative ratio of NH_3 and ND_3 adsorbed on Cu(100) is determined. In this way any uncertainties due to isotopic exchange of ND_3 with hydrogen on the chamber walls can be avoided.

The experiments on ammonia adsorption and photodesorption on an Ag film at near 10 K are carried out in a separate UHV chamber also described previously.[10] Basically, a sodium chloride film is deposited onto a sapphire substrate and a silver film is deposited on top of NaCl film at 25 °C. Deposition of the solid films at 25 °C as well as ammonia adsorption at low temperatures is monitored with a quartz-crystal microbalance. The focused ir beam is p-polarized and incident at 60° from the surface normal covering a surface area of about 5 mm^2. The time-of-flight distance is about 80 mm in this arrangement.

B. Adsorption of NH_3 on Cu(100)

The adsorption behavior of NH_3 on Cu(100) at 90 K was studied by thermal-desorption spectroscopy (TDS) and x-ray photoemission spectroscopy (XPS). XPS spectra as shown in Fig. 1 show no major chemical shifts in the core-level Cu($2p_{3/2}$,$2p_{1/2}$) and N($1s$) peaks due to NH_3 adsorption. The surface coverages (Θ) are determined from both the XPS intensity analysis and the thermal-desorption spectra. The TDS spectra in Fig. 2 indicate the presence of four different adsorbed states: solid (δ), multilayer (γ), and two chemisorbed states (β,α) The existence of these molecular species at 90 K is a function of coverage. In the submonolayer regime two chemisorbed states desorb at a heating rate of 6.5 ± 0.2 K sec^{-1} at 250 ± 10 K (α state) and 185 ± 10 K (β state), respectively. In the (2—3)-monolayer regime a physisorbed state desorbs at 132 ± 7 K (γ state), which for larger coverage is preceded by desorption from the solid phase at 105 ± 5 K. To extract desorption energies Q we assume that desorption is first order, according to the rate equation $r=\nu\exp(-Q/RT)$. The conventional choice of $\nu=10^{13}$ sec^{-1} gives for the respective desorption energies $Q_\delta=26\pm3$ kJ/mol, $Q_\gamma=32\pm3$ kJ/mol, $Q_\beta=45\pm5$ kJ/mol, and $Q_\alpha=63\pm6$ kJ/mol. On the other hand, we can take the heat of sublimation for solid NH_3, $Q=39$ kJ/mol,[17] and, assuming first-order kinetics, then calculate a pre-exponential factor from the peak in the TDS spectrum δ at $T=105$ K. We get $\nu\approx5\times10^{14}$ sec^{-1}. Assuming this value for all adsorption states gives their respective heats of adsorption as $Q_\gamma=35\pm4$ kJ/mol, $Q_\beta=52\pm5$ kJ/mol, and $Q_\alpha=70\pm7$ kJ/mol, respectively. Within $\pm10\%$, the two sets of estimates agree reasonably well. One might question whether desorption from a multilayer (γ and δ states) is indeed a first-order process. Rather, one would expect sublimation, like evaporation, to be a zeroth-order process. This is predicted for phy-

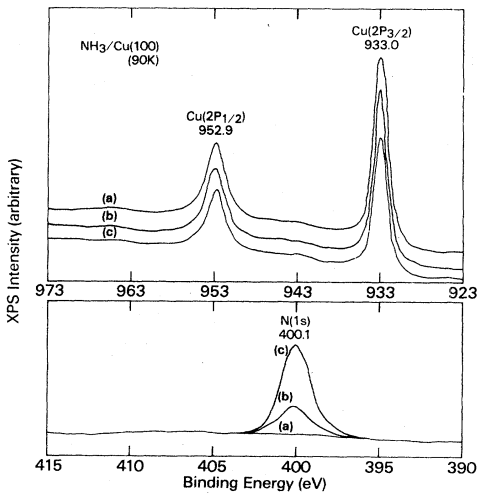

FIG. 1. X-ray-photoemission-spectroscopy spectra of NH_3 adsorbed on Cu(100) single crystal at $T=90$ K: (a) clean surface, (b) surface coverage about one monolayer ($\Theta=1$), (c) coverage about four monolayers ($\Theta=4$).

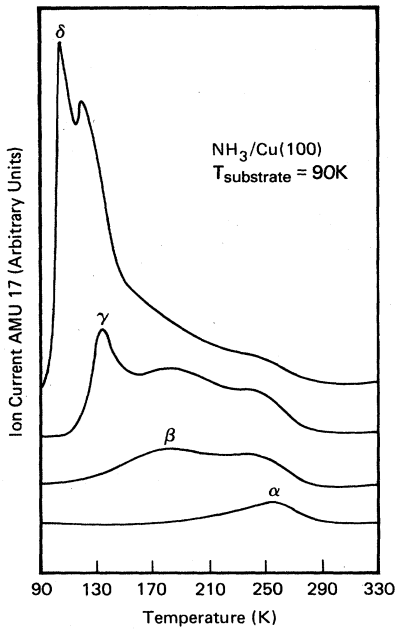

FIG. 2. Thermal-desorption spectra of NH_3 adsorbed on Cu(100) at 90 K at different coverages: $\Theta=0.4$, 0.8, 2, and 5, respectively. Heating rate 6.5 K/sec. Phase α,β: NH_3 chemisorbed on Cu(100), phase γ: NH_3 multilayers on top of chemisorbed NH_3 and phase δ: solid NH_3.

sisorbed multilayers in a mean-field model[18] and has also been observed experimentally in the Xe-W system.[19,20] For zeroth-order kinetics the TDS spectra have to be interpreted differently. Because in the photodesorption experiments only a very small fraction of a monolayer, of the order of 10^{-4}, is actually desorbed, the distinction between first and zeroth order for the physisorbed state is not crucial.

The vibrational spectrum of NH_3 adsorbed on Cu(100) has not been measured. In an electron-energy-loss—spectroscopy (EELS) study of NH_3/Cu(110), Lackey *et al.*[21] found, at low coverages, bands at 3360 and 3430 cm^{-1}, which merged into a broad band centered around 3400 cm^{-1} at more than 1 monolayer coverage. The latter was assigned to the ν_a stretching mode. The corresponding symmetric and antisymmetric N—H stretching modes for adsorbed ND_3 appeared at 2420 and 2520 cm^{-1}. No evidence of dissociative adsorption of NH_3 and ND_3 on the copper surface was observed. It was also suggested that the molecular adsorption involved the nitrogen lone-pair electrons interacting with the metal surface. Similar vibrational frequencies and configurations of interactions were also determined by EELS for NH_3 and ND_3 adsorbed on silver surfaces.[22]

From an analysis of the interaction of the closed shell, lone-pair ligand NH_3 with a Cu_5 cluster by Bagus *et al.*,[23] using the constrained space-orbital variational method (CSOV), it is deduced that formation of covalent chemical bonds is not particularly important for NH_3; the bonding can be viewed as electrostatic and arising because of the large NH_3 dipole moment, $\mu=0.81$ a.u. (1 a.u.$=2.54$ D) with N^-H^+ characteristics. The binding energy was found to be 0.92 eV ($=89$ kJ/mol). An on-top site-adsorption geometry was suggested with the nitrogen atom on top of a copper atom.

C. Photodesorption of NH_3 from Cu(100)

ir-laser-induced photodesorption (ir-LIPD) signals from a monolayer of ammonia, where species α, β, and some γ (just visible) are present, could be obtained by tuning the laser in the range of 3320 to 3370 cm^{-1} and applying a laser fluence larger than a threshold value of 4 mJ/cm^2. A time-of-flight signal is shown as curve (a) in Fig. 3. The TOF spectrum appears to be too broad to be fitted to a Maxwellian time-of-flight distribution, i.e.,

$$\frac{dN}{dt} \approx \left[\frac{t_0}{t}\right]^4 e^{-(t_0/t)^2}, \tag{1}$$

where $t_0=l(m/2k_BT)^{1/2}$ is the time that a particle of a mass m and energy k_BT needs to travel the distance l to the detector. For the effective translational temperature T_d estimated from the peak of the TOF spectrum, we get $T_d=80\pm25$ K. Curve (b) in Fig. 3 shows a time-of-flight signal from a multilayer with $\Theta=3.4$, obtained by tuning the laser to $\nu=3370$ cm^{-1}. It is again a rather broad spectrum for which a temperature of $T_d=90\pm25$ K can be estimated from the peak position t_m. Part of the spectral broadening can be attributed to the time constant of the mass spectrometer, which can shift the peak of the TOF spectrum to a later time, resulting in a lower translational temperature. Therefore, the estimated T_d at 80—90 K is very likely a lower limit. The spectral broadening can also be due to excessive noise and to difficulties in establishing the zero levels of the signal.

In Fig. 4 we show the frequency dependences of the

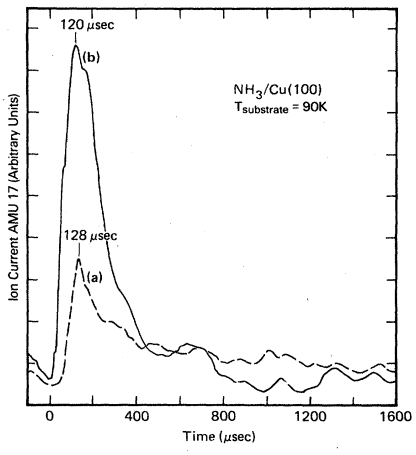

FIG. 3. Time-of-flight mass-spectrometer signals of NH_3 photodesorbed from Cu(100) at 90 K substrate temperature: (a) $\Theta=1$, $\nu_{laser}=3340$ cm^{-1}, and laser fluence $F_L=10$ mJ/cm^2, and (b) $\Theta=3.4$, $\nu_{laser}=3370$ cm^{-1}, and $F_L=10$ mJ/cm^2. The laser beam is p polarized and at a 75° angle of incidence. Sampling average of 20 desorption events.

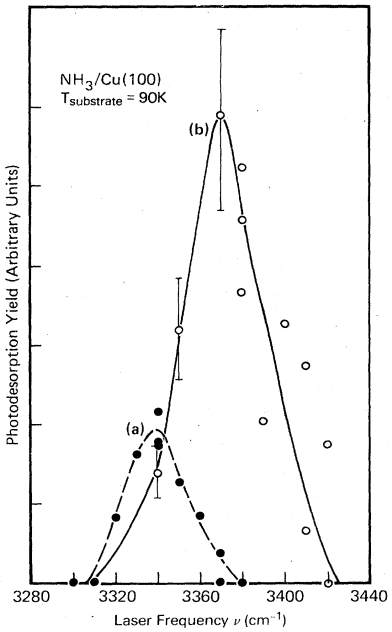

FIG. 4. ir-photodesorption yields of NH_3 adsorbed on Cu(100) at 90 K as a function of laser frequency: (a) $\Theta=1$ and $F_L=10$ mJ/cm^2, and (b) $\Theta=3.4$ and $F_L=10$ mJ/cm^2. Each data point is an average of mass-spectrometer signals due to 20 desorption events. Some error bars are also indicated.

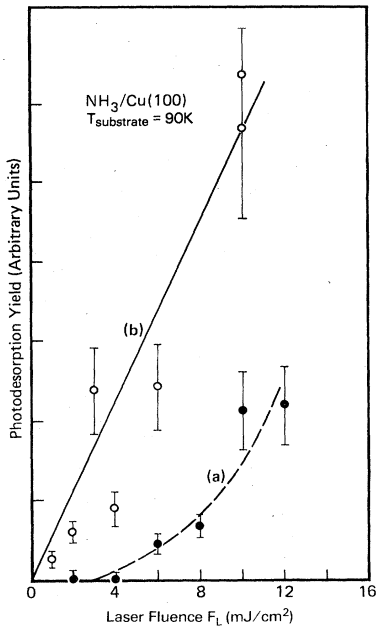

FIG. 5. Photodesorption yields of NH_3/Cu(100) at 90 K as a function of laser fluence taken at the maximum of the frequency dependence: (a) $\Theta=1$, $\nu=3340$ cm^{-1}, and (b) $\Theta=3.4$, $\nu=3370$ cm^{-1}. Sample average of 20 desorption events.

desorption yields for both the monolayer (dashed curve) and the multilayer (solid curve) situation at the same laser fluence. The statement in an earlier paper[16] that these curves were taken at different laser fluences is in error. It should be noted that peak heights, half-widths, and center positions are different for the two adsorbates. Figure 5 gives the dependence of the peak height as a function of laser fluence, showing that the yield from a monolayer is always less than that from a multilayer. We note that raising the laser fluence to more than 20 mJ/cm^2 causes the resonance features to diminish, indicating that direct heating of the copper substrate becomes efficient enough to desorb NH_3 thermally. It is possible that at this laser fluence, the increase in surface temperature can be greater than 35 K above T_s at 90 K to thermally desorb some physisorbed molecules due to substrate absorption of laser photons. Because the heat of adsorption for a (chemisorbed) monolayer $Q_\beta \approx 52$ kJ/mol is considerably larger than in a multilayer with $Q_\gamma \approx 35$ kJ/mol, one expects that the resonance behavior in the two situations disappears at different temperatures related roughly by $T_\gamma/T_\beta \approx Q_\gamma/Q_\beta$. This is indeed borne out by experiment.

The absolute photodesorption yields are difficult to determine. We irradiated the adsorbate at both the monolayer (with ν at 3340 cm^{-1}) and the multilayer (with ν at 3370 cm^{-1}) coverages with 500 laser pulses at $F_L=10$ mJ/cm^2 covering a sample area of 5×5 mm^2. This was done by translating the sample during the laser-irradiation period and examining the sample with XPS, which probes about the same surface area. No measurable changes in XPS intensities (within 10% uncertainty) due to laser photodesorption at these laser frequencies were observed, although no desorption signals by mass spectrometer could be detected after 50 pulses. Clearly, the amount of molecules desorbed from the surface is very small, possibly less than 10^{11} molecules/cm^2 per pulse, i.e., $<6\times10^{-7}$ molecules per incident ir photon. The desorption quantum yields per absorbed ir photon are estimated to be less than 5×10^{-4}. In contrast, decrease of NH_3 coverage on the Cu(100) surface by a single laser pulse at 532 nm and $F_L=20$ mJ/cm^2, which is quite strongly absorbed by the Cu substrate to cause laser-induced thermal desorption, is readily detected by XPS.

D. Photodesorption of NH_3 and ND_3 from Cu(100)

The composition of the gases co-adsorbed on the copper surface is directly determined by laser-induced thermal desorption with 532-nm light pulses. ND_3 is detected at 20 amu and NH_3 at 17 amu by the mass spectrometer. Figure 6 shows the TOF signals for a NH_3 and ND_3 (1:1) mixture thermally desorbed by a 532-nm light pulse. From the observed t_m, the translational temperature of desorbing particles, T_d is estimated to be about 300 K.

When a monolayer of this gas mixture is absorbed on Cu(100) at 90 K, the photodesorption signals due to resonance excitation in the (3320–3350)-cm^{-1} range are very weak. Therefore, the surface coverage was increased to about 2–3 monolayers. As shown in Fig. 7, both NH_3

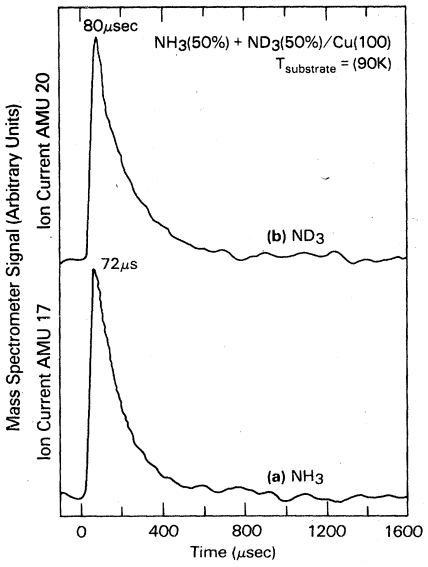

FIG. 6. Time-of-flight signals due to laser-induced thermal desorption of a NH_3-ND_3 (1:1) mixture adsorbed on Cu(100) at 90 K excited by 532-nm light pulses at 20 MW/cm^2, $\Theta=4$. Single-desorption events.

and ND_3 desorption are detected at $\nu=3370$ cm^{-1} and laser fluence $F_L=6$ mJ/cm^2. The relative desorption yields are about the same. Repetitive measurements show that within the relatively large experimental uncertainties, i.e., about $\pm 25\%$, there is no apparent isotope selectivity in the photodesorption of the isotopic co-adsorbates. Clearly, although only NH_3 molecules are initially excited by ir photons, either by direct vibrational energy transfer or by thermally assisted processes, the co-adsorbed ND_3 can be desorbed with almost equal probability as NH_3. It should be noted that an earlier study by Chuang[11,12] on C_5H_5N and C_5D_5N at about 2 monolayer coverages co-adsorbed on a KCl surface excited by CO_2 laser pulses also showed a lack of isotopic selectivity in the multiphoton-excited desorption. The new results demonstrate that a single-photon absorption cannot promote efficient separation of different ammonia (multilayer) isotope species from a Cu(100) surface by ir photodesorption either. The translational temperatures of the photodesorbed species, as estimate from TOF signals shown in Fig. 7, are about 75 ± 25 K.

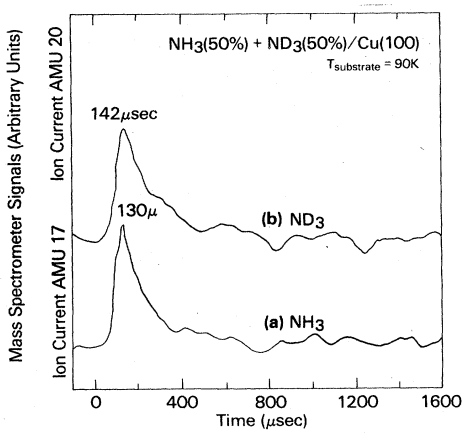

FIG. 7. Time-of-flight signals of NH_3 and ND_3 photodesorbed from Cu(100) at 90 K for a (1:1) mixture in the adsorbed phase: $\Theta=2.5$, $\nu=3370$ cm^{-1}, and $F_L=6$ mJ/cm^2. Sampling average of 20 desorption events.

E. Photodesorption of ND_3 on Cu(100)

The N—D stretching vibrational modes for adsorbed ND_3 on Cu(100) are expected to be in the (2400—2550)-cm^{-1} region. When the adsorbate at a monolayer or multilayer coverage is excited with laser pulses in this spectral region at $F_L=4$ mJ/cm^2 no significant photodesorption is detected by the mass spectrometer. We cannot produce more intense laser pulses because the laser approaches its tuning limits and the ir generating efficiency is quite low at or near 4 μm. The result suggests that ir photons at 4 mJ/cm^2 near 2500 cm^{-1} can excite adsorbed ND_3 molecules but cannot induce significant desorption by single-photon absorption. In contrast, we recall that physisorbed NH_3 molecules can be readily desorbed by ir photons at 3370 cm^{-1} with the same laser fluence. This should not be surprising because one ir photon at 2500 cm^{-1} can supply the molecule an energy equivalent to 30 kJ/mol, which is smaller than the adsorption energy of 35 kJ/mol for physisorbed ammonia, whereas the ir photon at 3370 cm^{-1} corresponds to 40 kJ/mol, enough to break the physisorption bond by single-photon absorption. The result further suggests that at 4 mJ/cm^2 the laser fluence is apparently inadequate in promoting multiphoton excitation to enhance desorption. This is also consistent with the observation that at this low fluence neither chemisorbed NH_3 nor ND_3 can be photodesorbed at $\nu=3340$ cm^{-1} or near 2500 cm^{-1}.

F. Photodesorption of NH_3 and ND_3 from Ag film

The 50-nm-thick silver film that we have prepared happens to be quite rough and not entirely continuous, possibly because of the rough underlying NaCl film deposited on the sapphire substrate. For NH_3 adsorbed on Ag film held at 60—90 K, laser-induced thermal desorption by direct substrate heating is clearly evident. Molecular desorption at a monolayer coverage can take place for fluence F_L as low as 2 mJ/cm^2 and independent of the laser frequency. The severe laser substrate-heating effect is most likely due to the roughness and discontinuity of the metal film. We therefore lower the substrate temperature and observe desorption due to resonance absorption of ir photons at $T_s\leq 15$ K. The results presented below are obtained at $T_s=10\pm 2$ K. A typical TOF signal for NH_3 on the Ag surface with $\Theta=2$ excited at $\nu=3390$ cm^{-1} and $F_L=3$ mJ/cm^2 is shown in Fig. 8. The translational temperature determined from t_m of the TOF signal is about 80 K. Thermal contribution from the direct laser substrate heating is not negligible because thermal desorption is detectable when the laser fluence is raised by only a factor of 2.5. Since some physisorbed NH_3 molecules desorb near 130 K, it is likely that at least part of the Ag surface is heated up to the 50-K range at $F_L=3$ mJ/cm^2. The desorption yield as a function of the laser frequency under

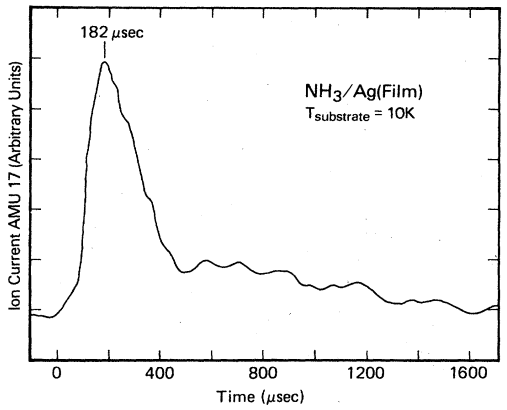

FIG. 8. Time-of-flight (TOF) signal of NH_3 photodesorbed from Ag film at 10 K with $\Theta=2$; $\nu=3390$ cm^{-1} and $F_L=3$ mJ/cm^{-2}. Note that the TOF distance is increased by a factor of 1.8, in comparison to the NH_3/Cu(100) system.

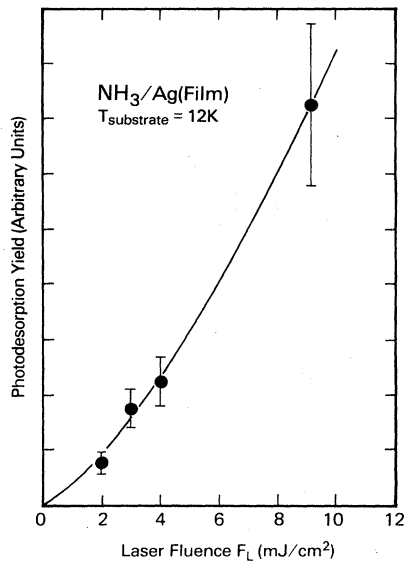

FIG. 10. Photodesorption yields of NH_3 adsorbed on Ag film at 12 K as a function of laser intensity: $\Theta=4$ and $\nu=3400$ cm^{-1}.

such an excitation condition and a substrate temperature of 10 K is shown in Fig. 9. At this surface coverage ($\Theta=2$), NH_3 desorption due to the photon absorption by both the physisorbed and the chemisorbed molecules (at lower vibrational frequencies) is quite evident. Namely, absorption of ir photons by the underlying chemisorbed layer can also induce some physisorbed molecules in the top layer to desorb. When the thickness of the molecular overlayer is increased, this effect is reduced, similar to that observed in the NH_3/Cu(100) system shown in Fig. 4(b), whereas at $\Theta=3.4$, desorption due to excitation in the chemisorbed layer ($\nu=3340$ cm^{-1}) is apparently less pronounced. Also, as in NH_3/ Cu(100), the desorption yield increases with the overlayer thickness in the higher-vibrational-frequency (physisorbed) region. The desorption yield as a function of laser fluence at a multilayer coverage $\Theta=4$ in NH_3/Ag film is shown in Fig. 10. The data point at $F_L=10$ mJ/cm^2 in the figure is due partly to the thermal desorption induced by the direct laser substrate-heating effect.

A NH_3-ND_3 (1:1) mixture is prepared and dosed onto Ag film at 10 K with a surface coverage of about 3—4 monolayers. The relative NH_3 and ND_3 surface concentrations are determined directly by laser-induced thermal desorption of the mixture with high-intensity ir laser pulses at $\nu=3500$ cm^{-1}, which is not in resonance with any vibrational bands of the adsorbed molecules. When the adsorbed NH_3 is excited at $\nu=3400$ cm^{-1} and $F_L=6$ mJ/cm^2, desorption of both NH_3 and ND_3 molecules is detected by the mass spectrometer. Within the relatively large experimental uncertainty (±25%), no significant isotope selectivity in the photodesorption is observed.

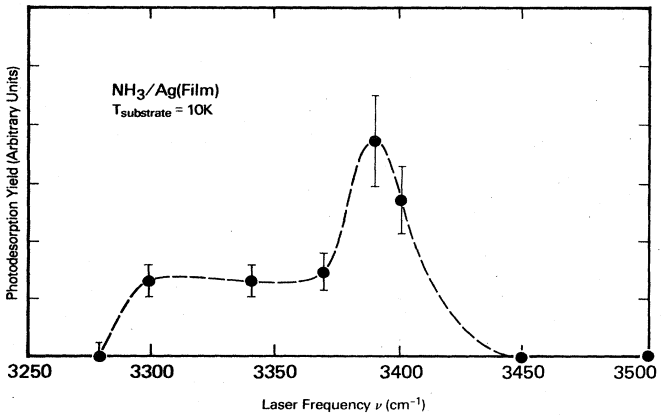

FIG. 9. Photodesorption yields of NH_3 adsorbed on Ag film at 10 K as a function of laser frequency: $\Theta=2$ and $F_L=3$ mJ/cm^2.

III. ANALYSIS AND DISCUSSION

A. Heating effects

In this section we will present a thorough discussion of the experimental data given in the preceding section. We will use previously developed theories[13–15] and also set up phenomenological models to find a quantitatively consistent picture. We base the initial discussion on the following facts: (i) the photodesorption yield from the chemisorbed monolayer is less than that from a physisorbed multilayer (ii) for a multilayer adsorbate the desorption yield increases with the overlayer thickness, (iii) the photodesorption yield per laser pulse is of the order of only 10^{-4} of a monolayer, and (iv) from an equal mixture of co-adsorbed NH_3 and ND_3 at two or more monolayer coverages, one photodesorbs about equal amounts of the two species, i.e., no enhanced molecular selectivity.

The last fact, in particular, suggests that the laser energy, initially resonantly coupled into NH_3, is rapidly degraded into thermal energy that is equally accessible to both species making the final desorption process independent of the initial excitation mechanism. This process has been termed resonant heating[14] or indirect heating.[11,12] Before we outline the mechanism of resonant heating, we present a phenomenological analysis of the data. We first note that the photodesorption yield Y is the total number of molecules desorbed per laser pulse of a given fluence. We assume that

$$Y \propto N_0(1-e^{-r_d t_L}) , \tag{2}$$

where N_0 is the number of molecules originally present on the surface area illuminated, r_d is the desorption rate constant, and t_L is the time over which desorption takes place which we might equate with the laser-pulse duration. Because $t_L \ll t_d = 1/r_d$ with $t_L = 6$ nsec for all experiments reported here, we immediately get

$$Y \propto N_0 t_L r_d . \tag{3}$$

The constant of proportionality includes the efficiency of the detector. Because XPS signals indicate that after 500 laser pulses less than about 10^{-1} of a monolayer is desorbed (i.e., $Y < 2\times 10^{-4} N_{\text{mono}}$), we can get as a crude upper limit for the desorption-rate constant

$$r_d < 2\times 10^{-4} \frac{N_{\text{mono}}}{N_0} t_L^{-1} \approx 3\times 10^4 \text{ sec}^{-1} , \tag{4}$$

where N_{mono} is the number of molecules in a monolayer. A smaller photodesorption yield for a monolayer of NH_3 can be traced to a smaller desorption-rate constant. Figure 5 suggests that at a fluence of 10 mJ/cm^{-2}, $r_d^{(b)} \sim 3 r_d^{(a)}$. If we use a Frenkel-Arrhenius parametrization for the rate constant,

$$r_d = \nu e^{-Q/RT} , \tag{5}$$

we obtain

$$3\frac{\nu_\beta}{\nu_\gamma} \exp\left[\frac{Q_\gamma}{RT_\gamma} - \frac{Q_\beta}{RT_\beta}\right] \approx 1 . \tag{6}$$

Note that the superscripts (b) and (a) are related to the two graphs of Fig. 4, the multilayer (b) and the monolayer (a) situation, respectively, while subscripts β and γ are related to the different phases present on the surface as a function of coverage and with different heats of adsorption Q_β and Q_γ determined by conventional TDS spectroscopy (see Sec. II B). Assuming that ν_β and ν_γ do not differ significantly, one would estimate that $T_\beta/T_\gamma \approx Q_\beta/Q_\gamma \approx 1.5$. The time-of-flight spectra in Fig. 2 suggest that $T_d(\beta) \approx 1.14 T_d(\gamma)$. However, it is still instructive to insert some numbers; e.g., for $\nu = 5\times 10^{14}$ sec^{-1} and $Q_\gamma \approx 35$ kJ/mol, one gets $T_\gamma < 177$ K; for $\nu = 10^{13}$ sec^{-1} and $Q_\gamma = 32$ kJ/mol, one gets $T_\gamma < 194$ K. Desorption temperatures for the chemisorbed monolayer are higher yet by some 50% according to this argument. It is very improbable that the time-of-flight measurements are so slow that their peak corresponds to only half of these estimated desorption temperatures. Two possible explanations come to mind: (i) Because of the high resonant heating rate suggested by these estimates, namely, a temperature rise of some 120 K in $t_L = 6\times 10^{-9}$ sec, slow particles are preferentially desorbed. Such a scenario has been suggested by Tully[20] and is claimed to explain laser-induced thermal-desorption data of CO from copper surfaces.[6] (ii) It is possible that the desorbing molecules have about half of their energy stored in rotation. With the rotational temperature of NH_3 being $T_{\text{rot}} = 11$ K, we find that 100 K worth of energy leads to a rotational quantum number $J \approx 2$–3. At this stage these scenarios are purely speculative.

B. Model calculations: Phonon damping

We now turn to explicit calculations of photodesorption rates and briefly outline the theory of photodesorption of molecules by resonant laser-molecular vibrational coupling,[13] including resonant heating.[14] Physisorption and weak chemisorption of a molecule onto a surface can be adequately described by a surface potential. Molecules trapped into their bound states form the adsorbate. Because the energy $\hbar\Omega$ of the vibrational mode of the molecule into which the laser couples is typically much larger than the energy difference between adjacent energy levels in the surface potential $(E_{i+1} - E_i)$, one can decouple these degrees of freedom. Assuming that the lowest few vibrational states of the molecule are harmonic, we can write the energy of a molecule in its vth internal vibrational state and in an energy level E_i in the surface potential $E_i^v \approx E_i + (v + \frac{1}{2})\hbar\Omega$. The theory of photodesorption of molecules by resonant laser-molecular vibrational coupling is based on a master equation:[13]

$$\frac{d}{dt} n_i^v(t) = \sum_{v'=0}^{\infty} \sum_{i'=0}^{i_{\max}} [(\mathscr{L}_{ii'}^{vv'} + P_{ii'}^{vv'}) n_{i'}^{v'}(t) - (\mathscr{L}_{i'i}^{v'v} + P_{i'i}^{v'v}) n_i^v(t)] - \sum_{v'=0}^{\infty} (P_{ci}^{v'v} + Q_{ci}^{v'v}) n_i^v(t) \tag{7}$$

(see Ref. 13). Here, $n_i^v(t)$ is the time-dependent occupation function for a molecule in a state i of the surface potential and the vth excitation of the relevant internal vibration mode.

In master equation (7), $\mathscr{L}_{ii'}^{vv'}$ is the rate at which the coupling of the molecular dipole to the electromagnetic field of the laser causes transitions up or down the vibrational excitations; we note that it is only nonzero for $i = i'$ and $v = v' \pm 1$. $P_{ii'}^{vv'}$ is the transition rate between bound states mediated by one-phonon absorption and emission processes calculated according to Fermi's golden rule from a microscopic Hamiltonian. $P_{ci}^{v'v}$ and $Q_{ci}^{v'v}$ are the transition rates from a bound state (i,v) into all continuum states, with the first mediated by phonons and the second being an elastic tunneling process. These two terms lead to desorption. More details can be found in Ref. 13, where the transition probabilities have been calculated for a surface Morse potential. A schematic picture of all processes involved is given in Fig. 1 of Ref. 13.

The above harmonic approximation needs some justification; e.g., for NH_3 the anharmonicity amounts to about 39 cm^{-1}. This would imply that a laser with a spectral

resolution better than 1 cm^{-1} cannot populate the $v=2$ state. However, we recall that the physisorbed species is bound by less than $\hbar\Omega$, so that a single-photon excitation is sufficient to lift the molecule into a state degenerate with the continuum. As for the chemisorbed surface species, we note that the coupling to the solid typically induces a linewidth of the order 10—50 cm^{-1} that will, in most systems, offset the effects of the anharmonicity. Moreover, in the low-intensity region (i.e., below saturation) the laser-induced desorption rates are not very dependent on the highest vibrational level accessed by the laser, as can be inferred from the rising parts of the yield curves in Figs. 11 and 12 and Fig. 3 of Ref. 13.

At low temperatures an adsorbed molecule will be in the ground state of energy

$$E_i^v = E_0^0 = E_0 + \tfrac{1}{2}\hbar\Omega \ . \tag{8}$$

Upon absorption of a laser photon the molecule will be in a state E_0^1 from which it can either absorb more photons to go up to a higher v or emit a phonon of energy $\hbar\omega$ such that $E_i^0 = E_0^1 - \hbar\omega$. It is then in an excited state of the surface potential from which it can cascade down to $i=0$, emitting more phonons and thus heating up the solid. This process we have termed resonant heating.[14] As long as the coupled gas-solid system is in local equilibrium, resonant heating can be quantified by coupling the master equation to Fourier's law of heat conduction[14]

$$\frac{\partial T}{\partial t} - \chi\nabla^2 T = 0 \ , \tag{9}$$

where χ is the thermal diffusivity. For a heat source at the surface, Eq. (9) has to be supplied with a radiative boundary condition

$$\left.\frac{\partial T}{\partial Z}\right|_{z=0} = \frac{N_a}{\lambda}\dot{U} \ , \tag{10}$$

$$\dot{U} = \sum_{\mathbf{p},\sigma} \hbar\omega_{\mathbf{p}\sigma} \frac{dn_{\mathbf{p}\sigma}}{dt} \ , \tag{11}$$

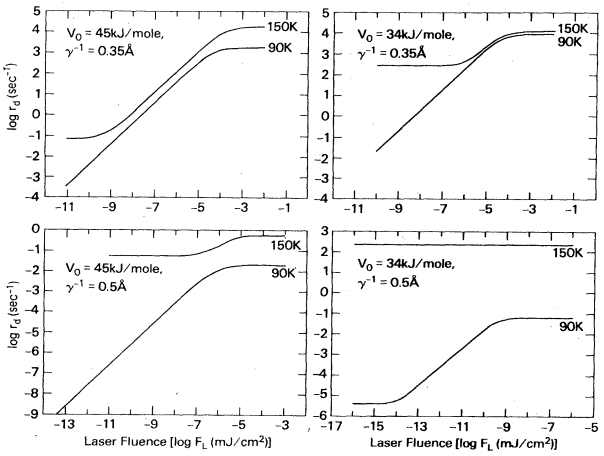

FIG. 11. Desorption rates r_d as a function of laser fluence F_L for different parameters calculated from Eq. (7).

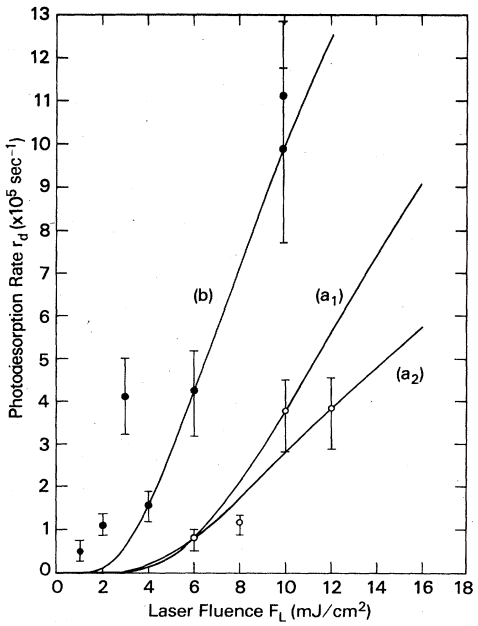

FIG. 12. ir-photodesorption rate r_d for NH_3 on Cu(100) vs laser fluence $F_L = It_L$. I is the incident laser intensity and t_L the duration of the laser pulses, ≈ 6 nsec, based on Eq. (7). The angle of incidence is 75°, the effective charge q given below corresponds to laser linewidths $\Gamma_L = 3.0$—1.0 cm^{-1}. Curve b: $Q=35$ kJ/mol, $\nu = 5\times10^{14}$ sec^{-1}, $R = 4.6\times10^{10}$ sec^{-1}, $q=(2$—$4)e$. Curve a_1: $Q=51$ kJ/mol, $\nu = 5\times10^{14}$ sec^{-1}, $R = 2.7\times10^{11}$ sec^{-1}, $q=(4.2$—$7.8)e$. Curve a_2: $Q=51$ kJ/mol, $\nu = 5\times10^{14}$ sec^{-1}, $R = 2.6\times10^{11}$ sec^{-1}, $q=(5$—$9)e$.

where $\dot{U}$ is the energy supply during the desorption process, with $n_{\mathbf{p}\sigma}(t)$ the nonequilibrium occupation function for phonons of wave vector $\mathbf{p}$ and mode σ. Its change is due to the bound-state—bound-state transitions in the master equation; details are worked out in Ref. 14. N_a is the number of adsorbed molecules.

We have calculated the photodesorption rates from the model based on master equation (7), coupled to the heat, Eq. (9). We recall that the diagonalization of the matrix of transition probabilities on the right-hand side of (7) yields a set of eigenvalues λ_j, so that the solution of Eq. (7) gives

$$n_i^v(t) = \sum_j S_{ij}^v e^{-\lambda_j t} \ . \tag{12}$$

It turns out that one of the eigenvalues is much smaller than the others and occurs in Eq. (12) with a much larger weight, S_{ij}^v. It is therefore identified as the rate constant r_d. It is obviously a function of temperature, the latter rising during the course of desorption due to resonant heating. The input parameters of the theory are depth V_0 and range γ^{-1} of the surface Morse potential, the resonant frequency Ω of the vibrational NH_3 mode excited by the laser, the dynamic dipole moment or effective charge $Q = \partial\mu/\partial x$ of the molecule, and the index of refraction of the metal which we take to be very large.

In Fig. 11 we give the photodesorption rates as calculat-

ed from (7) as a function of laser fluence F_L for different potential parameters and temperatures. We get rates of the order of 10^4 sec^{-1} at *much too low fluences*. In the linear regime the laser-induced transition $\mathscr{L}_{ii'}^{vv'}$ is the rate-determining step. It must be stressed that for both monolayer and multilayer desorption, r_d is linear in F_L in this regime, despite the fact that for a multilayer a one-photon excitation is sufficient, whereas a monolayer adsorbate demands absorption of at least two photons. The reason is simply that with $\mathscr{L}_{ii'}^{vv'}$ being the rate-determining step the level $v=1$ in the monolayer is emptied out much faster by the phonon-induced transitions $P_{ii'}^{vv'}$. This is quite different from the gas-phase situation, where this loss mechanism is obviously absent, although energy transfer to rotational or other vibrational degrees of freedom is possible. Coherent two-photon excitations would, of course, produce a dependence like F_L^2, but then they are negligible whenever incoherent two-photon processes [included with all other multiphoton cascades in Eq. (7)] are possible. This point will be demonstrated in greater detail in a forthcoming publication in which we will calculate all fourth-order processes; there we will show that coherent one-photon—one-phonon excitations are indeed sometimes of importance. We will return to this point later.

For the highest fluences, r_d becomes independent of F_L because now the tunneling rates Q_{ci} and P_{ci} into the continuum are the rate-determining steps. The reason why such low fluences are sufficient in the theory can be traced back to the fact that the loss mechanism $P_{ii'}^{vv'}$ (whereby a molecule de-excites by creating phonons in the solid) are too weak. They can be enhanced by a stronger coupling to the solid, i.e., by reducing the range of the surface potential γ^{-1}, as clearly demonstrated in Fig. 11. *This brings us then to a necessary modification of the theory.* It was originally conceived to describe photodesorption of molecules from insulators such as CH_3F from NaCl.[7,8,13] Dealing now with a metal, we should note that the molecule, internally or externally excited at the surface of a metal, can lose its energy not only by creating phonons but also by direct coupling into the electronic degrees of freedom. In particular, for the chemisorbed state this should be a rather efficient energy-loss mechanism.

C. Model calculations: Electronic damping

To account for electronic losses we have set up a phenomenological version of the master equation. We first recall from our earlier work that below saturation, phonon transitions within the surface potential, i.e., the rates $P_{ii'}^{vv'}$, are very fast and basically keep a thermal occupation of the i states throughout the desorption process. With the energy of a molecule in state i,v being given by

$$E_i^v = E_i + (v+\tfrac{1}{2})\hbar\Omega \ , \tag{13}$$

where E_i is the energy level in the surface potential and Ω is the vibrational frequency of the molecule into which the laser couples, we can then write[15]

$$n_i^v(t) = a_v(t) e^{-\beta E_i} \Big/ \sum_j e^{-\beta E_j} \ , \tag{14}$$

where $\beta=(k_B T)^{-1}$. Inserted in Eq. (7), one can derive a set of equations for $a_v(t)$, namely,

$$\frac{da_v}{dt} = \sum_{v'} (L^{vv'} + R^{vv'}) a_{v'} - \sum_{v'} (L^{v'v} + R^{v'v}) a_v - R_d a_v \ , \tag{15}$$

where

$$R^{vv'} = \sum_{i,i'} e^{-\beta E_{i'}} (P_{ii'}^{vv'} + R_{ii'}^{vv'}) \Big/ \sum_j e^{-\beta E_j} \ , \tag{16}$$

is the thermally averaged loss rate due to phonons ($P_{ii'}^{vv'}$) and electrons ($R_{ii'}^{vv'}$). We will treat $R^{vv'}$ as a phenomenological parameter. We also define

$$R_d^v = \sum_{v',i} e^{-\beta E_i} (P_{ci}^{v'v} + Q_{ci}^{v'v}) \Big/ \sum_j e^{-\beta E_j} \tag{17}$$

as the rate constant for the desorption channel. As long as we are below saturation, we can neglect the terms with $v' \neq v$ so that R_d^v becomes the thermal-desorption rate R_d independent of v, for which we assume the Frenkel-Arrhenius parametrization.

With each transition due to $R_{ii'}^{vv'}$ and $P_{ii'}^{vv'}$, energy is given to or (much less likely) taken from the solid. This occurs at a rate (per adsorbed molecule)

$$\dot{U}(t) = \sum_{i,i'} \sum_{v,v'} (E_i^v - E_{i'}^{v'}) (R_{i'i}^{v'v} + P_{i'i}^{v'v}) n_i^v(t) \ . \tag{18}$$

In order to simplify Eq. (15) we recall that the phonon-induced transitions in each well, i.e., $P_{i'i}^{v'v}$, are the fastest in the system. We can therefore argue that the transitions $(iv) \rightarrow (i'v')$ (i.e., $R_{i'i}^{v'v} + P_{i'i}^{v'v}$, with $v \neq v'$) are immediately followed by the fast cascade of phonon-emission processes $(i'v') \rightarrow \cdots \rightarrow \cdots \rightarrow (0,v')$ and that the net energy supplied to the solid in this sequence is $E_i^v - E_0^{v'}$. This should be inserted into Eq (18) instead of $E_i^v - E_{i'}^{v'}$, with simultaneous exclusion of the terms with $v=v'$ in the summation. Now we can again invoke Eq. (13); observe that due to the exponential factor $e^{-\beta E_i}$, no serious error is made replacing $E_i^v - E_0^{v'}$ by $E_0^v - E_0^{v'} = \hbar\Omega(v-v')$, and finally we get

$$\dot{U}(t) = \hbar\Omega \sum_{v,v'} (v-v') R^{v'v} a_v(t) \ . \tag{19}$$

Obviously, $R^{v'v}$ has to be nonsymmetric; it indeed must satisfy detailed balance (assuming instantaneous thermalization of electrons in the metal),

$$R^{v'v} e^{-\beta\hbar\Omega v} = R^{vv'} e^{-\beta\hbar\Omega v'} \ . \tag{20}$$

$\dot{U}(t)$ is the rate with which the energy is given to the solid due to a de-excitation of a vibrationally excited molecule. The total energy rate for N_a adsorbed molecules is then $N_a \dot{U}(t)$. It leads to a temperature rise that is partially compensated by heat conduction into the solid controlled by Fourier's law, Eq. (9), with boundary conditions Eq. (10). This equation can be solved analytically, but because temperature also appears in Eq. (15) via the thermal-desorption rate R_d, Eqs. (15) and (9) have to be solved self-consistently, leading to what has been termed resonant heating via laser-adsorbate coupling.[14]

We briefly examine the rate equations for the multilayer situation where we can restrict ourselves to $v=0$ and 1. Take $L^{01}=L$, $R^{01}=R$, and assume $R^{10} \approx 0$, im-

plying that the electronic degrees of freedom of the solid do not supply energy into a $v=0$ to $v=1$ transition in the molecule. We then get for the rate equations

$$\begin{bmatrix}\dot{a}_0\\ \dot{a}_1\end{bmatrix}=\begin{bmatrix}-L-R_d & L+R\\ L & -L-R-R_d\end{bmatrix}\begin{bmatrix}a_0\\ a_1\end{bmatrix}, \tag{21}$$

which, of course, can be solved explicitly by matrix diagonalization to yield

$$a_i(t)=\sum_j S_{ij}e^{-\lambda_j t}, \tag{22}$$

where the eigenvalues are

$$\lambda_1=R_d,\quad \lambda_2=R_d+R+2L, \tag{23}$$

and the weights S_{ij} follow from the initial conditions. From the experience with the cascade model,[13–15] we know that the slower (thermal) rate λ_1 determines the desorption process, whereas the faster λ_2 will aid in resonantly heating the solid.

For the increase in surface temperature one can find an approximate solution

$$\Delta T=\frac{2\hbar\Omega\sqrt{\chi}N_A}{\sqrt{\pi}\lambda}\frac{RL}{R+2L}\times[\sqrt{t}\,\Theta(t_L-t)+(\sqrt{t}-\sqrt{t-t_L})\Theta(t-t_L)], \tag{24}$$

where $\lambda=C_V\chi/V_m$, and t_L is the duration of the laser pulse. The prefactor in Eq. (24) for Cu is about $2.26\times10^{-5}\Theta$ (Θ being the surface coverage):

$$L=\frac{q^2(m_1+m_2)}{\epsilon_0 c m_1 m_2\hbar\Omega}\left[\frac{2n_r\sin\phi}{n_r+[1+(1-1/n_r^2)\tan^2\phi]^{1/2}}\right]^2\times\frac{1}{t_L\Gamma_L}F_L, \tag{25}$$

where m_1 and m_2 are the masses associated with the molecular dipole, c is the velocity of light, and q is the effective charge. ϕ is the angle of incidence of the laser with respect to the surface normal, assuming that the dipole is perpendicular to the surface. n_r is the refraction index. For a metal we set $n_r\gg1$.

To try some numbers, we assume a linewidth of the $v=1$ level of 0.5 cm^{-1}. This corresponds to a damping $R\approx10^{11}$ sec^{-1}, leading, for a fluence of $F_L=10$ mJ/cm^2 and at monolayer coverage $\Theta=1$, to a maximum temperature rise of only 25 K. This temperature rise could cause a small fraction of physisorbed molecules to desorb, but not chemisorbed species. Here we assumed an effective charge on the NH_3 dipole $q\sim0.4e$ suggested by calculations of $\partial\mu/\partial x$ in the free molecule. If q is reduced at the surface to account for the shift in frequency, then F_L must be increased by the square of the reduction factor.

We recall from the earlier discussion around Eq. (6) that thermal desorption would necessitate temperatures of the order $T_\gamma\approx180$–190 K and $T_\beta\approx1.5T_\gamma$. This would imply that the $v=1$ linewidth in the physisorbed state would correspond to an electric loss rate of the order of 10^{10}–10^{11} sec^{-1}, whereas for the chemisorbed state either q is increased or R is increased to 2×10^{11} sec^{-1}, both possibilities actually being reasonable. A set of r_d-vs-F_L curves that seem a reasonable fit to the experimental results is given in Fig. 12. Note that very effective heating in the chemisorbed state leads to a nonlinear dependence of r_d on F_L. We note that the effective charge on the NH_3 dipole is typically $q\approx(2$–$7)e$ to fit the data. This should be interpreted as an effective increase in the electric field strength at the surface by that factor rather than an additional polarization of the adsorbed molecule. In Fig. 13 we show the fluence dependence of the maximum surface temperature during the desorption processes.

The fits presented in Fig. 12 are such that the photodesorption rate is $r_d\approx10^6$ sec^{-1} for $F_L=10$ mJ/cm^2 for the physisorbed system. Because we only have an upper limit on r_d from experiment, we might also take $r_d\sim10^4$ sec^{-1}; the resulting fits are indistinguishable for about the same Q, but for R smaller by about 50%. It thus seems that resonant photodesorption, including resonant heating, can produce an explanation of the data, except for the fact that the time-of-flight spectra indicate too low a translational temperature. If, indeed, time zero in the time-of-flight signals is known well enough to determine temperatures to within 25 K, then it seems necessary to consider additional mechanisms to take up energy. This seems to us to be in rotational excitation of desorbing particles. As NH_3 molecules interact with each other via hydrogen bonds, it seems reasonable that, in that breakage, some angular momentum is generated on the molecule. With the rotational temperature of NH_3 being $T_{rot}\approx11$ K, the excess energy between the theoretical (170–200 K) and the experimental (90±25 K) would produce rotations with $J\approx2$ from the physisorbed state and $J\approx2$–3 from the chemisorbed state. A possible alternative explanation of the low translational temperature observed could stem from the high heating rates which, according to Tully,[20] result in preferential desorption of slow particles.

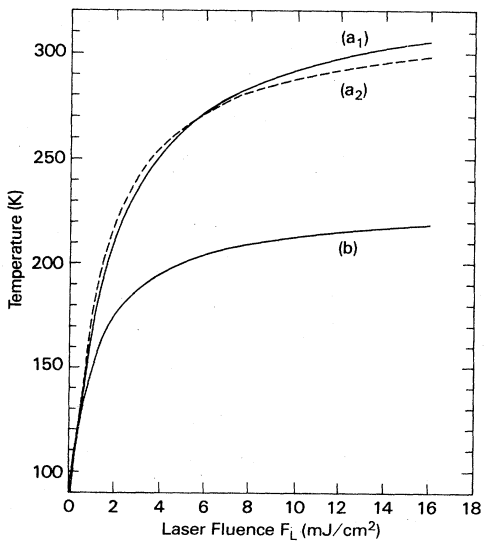

FIG. 13. Maximum temperature rise used for Fig. 12 with the maximum rise from Eq. (24) using $t=t_L=6$ nsec.

D. Frequency dependence

We return to Fig. 4, depicting the frequency dependence of the photodesorption yield and thus the resonant character underlying the desorption process. In Table I we have compiled vibrational frequencies of NH_3 and ND_3 in the gas, liquid, and solid phases, and adsorbed on silver and copper substrates. It is obviously the symmetric ($\nu_{s,\,gas}=3377$ cm^{-1}) or the antisymmetric (degenerate) ($\nu_{a,\,gas}=3414$ cm^{-1}) stretching modes of NH_3 into which the laser couples. The monolayer results [curve (a) of Fig. 4] suggest a resonance centered at $\nu=3340$ cm^{-1} with a full width at half maximum of about 33 cm^{-1}. This is very close to the gas-phase value of the symmetric stretching mode, which on Ag(110) (Ref. 22) is actually shifted downward by 20 cm^{-1}. It is thus very likely that the observed resonance is indeed due to the photoexcitation of the symmetric stretching mode. We note that in a monolayer, NH_3 is likely adsorbed perpendicular to the surface, with the N on top of a Cu so that the dynamic dipole moment due to ν_s is also perpendicular to the surface and thus infrared active. On the other hand, for ν_a the

TABLE I. Vibrational frequencies (in wave numbers) of fundamental modes of NH_3 in different states. NA indicates data not available.

	R_{xy}[a]	$\nu(M\text{-}N)$[b]	$\delta_s(NH_3)$[c]	$\delta_a(NH_3)$[d]	$\nu_s(NH_3)$[e]	$\nu_a(NH_3)$[f]	Remarks, references
NH_3 (gas)			950	1628	3337	3414	G. Herzberg, *Bd. II Molecular Spectra and Molecular Structure* (Van Nostrand, Princeton, 1945); K. Nakamoto, *Infrared and Raman Spectra of Inorganic and Coordination Compounds* (Wiley, New York, 1978)
ND_3 (gas)			748	1191	2419	2555	
NH_3 (liquid)			1032	1628	3250	3382	J. Corset, P. V. Huong, and J. Lascombe, Spectrochim. Acta **24A**, 1385 (1968)
ND_3 (liquid)	NA	NA	NA	NA	NA	NA	
NH_3 (solid)	360		1060	1646	3223	3378	F. P. Reding and D. F. Hornig, J. Chem. Phys. **19**, 594 (1950)
ND_3 (solid)	270		815	1196	2318	2500	
NH_3/Ag(110)							
Chemisorbed	430	430	1050	1640	3320	3400	EELS
Second layer	340		1100	1630	3320	3390	J. L. Gland, B. A. Sexton, and
Multilayer	400		1070	1630	3320	3388	G. E. Mitchell, Surf. Sci. **115**, 623 (1982)
ND_3/Ag(110)							
Chemisorbed	210		825		2370	2530	
Second layer	260		860	1190	2370	2510	
Multilayer	310		830	1146	2400	2510	
NH_3/Cu(110)							
Low coverage	560		1150	1600	3360	3430	EELS
High coverage	560		1130	1600	3400	3400	ν_s,ν_a Not resolved
ND_3/Cu(110)			870	1190	2420	2520	D. Lackey, M. Surman, and D. A. King, Vacuum **33**, 867 (1983)
NH_3/Ag film							
Multilayer			1075				Photoacoustic measurements H. Coufal, T. J. Chuang, and F. Träger, J. Phys. **44**, 297 (1983)
NH_3/Cu(100)							CO_2-LIPD absorption-desorption spectra
Multilayer			1056				I. Hussla and T. J. Chuang, Ber. Bunsenges. Phys. Chem. **89**, 294 (1985)
NH_3/Cu(100)							
Low coverage					3340		ir-LIPD, this work
Multilayer					3340	3370	Absorption-desorption spectra
NH_3/Ag film							
Multilayer					3320	3390	ir-LIPD, this work Absorption-desorption spectra

[a]Rotation about axis in x-y plane, also called ρ_r (NH_3).
[b]Also called outer mode or adsorbate mode.
[c]Bending mode, symmetric.
[d]Bending mode, asymmetric; also called degenerated.
[e]Stretching mode, symmetric.
[f]Stretching mode, asymmetric; also called degenerated.

dynamic dipole moment should be at right angles with respect to the molecular symmetry axis and thus to the surface normal. Image effects will thus render it more or less infrared inactive. The large linewidth (33 cm^{-1}) of this absorption-desorption band may be due to the inhomogeneous broadening of the two different chemisorbed states α and β which are present at a monolayer coverage and may have different vibrational frequencies for the symmetric stretching mode.

Turning next to the multilayer situation [curve (b) of Fig. 4], we note that molecular orientation induced by the surface should largely disappear, so that ν_a will also become ir active. This latter change is enhanced by the diminishing image charge effects as one moves into second and third overlayers. As more layers are adsorbed, ν_s and ν_a will approach their values in solid NH_3, namely 3323 and 3378 cm^{-1}, respectively. The observed photodesorption peak at 3370 cm^{-1} for the adsorbed multilayer is thus likely due to the excitation of the antisymmetric mode. Whereas for a monolayer this mode is ir active, for a multilayer with molecules pointing in all directions the laser couples to both symmetric and antisymmetric modes. The oscillator strength at ν_a does not differ very much from that at ν_s for ammonia in the gas phase.[24,25,26] This is also true for the adsorbed multilayer phase, e.g., in NH_3/Ag(110) (Ref. 22) or NH_3/Cu(110).[21] However, more ir energy is absorbed in the multilayer situation simply because the laser interacts with more molecules, which results in a higher desorption yield. Furthermore, if the first chemisorbed layer does not change appreciably in the vibrational frequency with the presence of two additional physisorbed layers, one would expect the multilayer spectrum to be a composite of both the ν_s and ν_a components. This is observed more clearly in the photodesorption spectrum of NH_3 at $\Theta=2$ adsorbed on Ag film (see Fig. 9). It would be very useful to carry out a detailed infrared-absorption-reflection spectroscopic measurement to determine the coverage dependence of the ν_s and ν_a modes in order to verify these assignments. In any event, we have demonstrated how ir photodesorption can be used to obtain ir-absorption—desorption spectra of adsorbates with the high-frequency resolution of an infrared laser.

IV. SUMMARY AND PERSPECTIVES

We have presented arguments based on model calculations that the *resonant* or *indirect* heating can result mainly from electronic damping mechanisms for molecules adsorbed on metal surfaces. We have also provided experimental evidence to show that thermally assisted processes, including *direct* and *resonant* (or *indirect*) heating effects, play a very important role in determining the ir-photodesorption yields. It should be emphatically pointed out, however, that thermal effects alone cannot account for all the major observations for the ir-excited desorption phenomenon, in particular, the low desorption yields and the low translational energies of desorbed particles as calculated from the time-of-flight spectra. If indeed the *resonant* or *indirect* heating is capable of raising the local surface temperatures to $T_\gamma=135$ K for desorbing the physisorbed species, and to $T_\beta=175$ K for the chemisorbed species, then the observed photodesorption yield ($<2\times10^{-4}$ monolayer per pulse) should be much higher and the observed translational temperatures 90 ± 25 K should be much closer to T_γ or T_β. Since this is not the case, we therefore suggest that the desorbing species may be in internally excited states, most likely in vibrational and rotational modes. This internal excitation, not necessarily the original vibration excited by the laser, may be acquired via the rapid inter- and intra-molecular-energy transfer processes in the adsorbed molecular layers. Internal excitation, in particular the rotational excitation, may also take place during the rapid heating and desorption process. Therefore, it is essential to determine the internal energy distributions before and after the molecules are desorbed into the gas phase. This is a difficult experiment to perform but it can definitely yield tremendous insight into the desorption dynamics.

Furthermore, the velocity distribution of the desorbed particles should be more clearly determined and checked as to whether it obeys a Maxwell-Boltzmann distribution. If it does, the translational temperature can be compared with the vibrational and rotational temperatures, if they are available, and one can determine the degree of surface accommodation. In order to obtain a complete picture, quantitative measurements of the photodesorption yields are also necessary. As far as the theory is concerned, the evaluation of the effective dipoles influenced and/or enhanced by the surface electromagnetic fields, and realistic estimates of the inter- and intra-molecular vibrational relaxation rates, are essential for microscopic understanding and modelings. Removing the harmonic assumption for the molecular vibration to take into account the anharmonicity in the molecular potential should also be very useful.

As to the future of the photodesorption of molecules by resonant laser-molecular vibrational coupling, there is no doubt that extensive experimental and theoretical work is still needed before a complete understanding of the phenomenon is achieved. If molecular selectivity and isotope separation are the goal, our analysis suggests that intermolecular energy transfer and thermal effects, including the direct and indirect (or resonant) heating, must be minimized. Thus, one should choose highly-ir-transparent or -reflective solids and good thermal-conducting materials as substrates, the latter to allow the energy deposited via resonant heating into the surface of the solid to be dissipated rapidly. It should also be helpful to keep the substrates at very low temperatures in order to decrease the thermal desorption rates. Low surface coverage (in the submonolayer range) could also reduce lateral intermolecular interactions. For molecular systems with relatively weak intermolecular interactions and large differences in vibrational frequencies between different isotopic species, it might be possible to observe the isotope effects in the ir photodesorption. From this reasoning, H_2 and D_2 appear to be a good system to investigate both experimentally and theoretically.

Note added in proof. Recently, we achieved LIPD of physisorbed NH_3 from Cu(100) single crystal via resonant pulsed CO_2 laser excitation of the symmetric deformation mode of δ_s.[27] In this case photofragmentation and pho-

toionization at increased laser intensities are also observed.

ACKNOWLEDGMENTS

This work was supported in part by grants from the Natural Sciences and Engineering Council of Canada. We would like to thank J. Goitia and J. Escobar for technical assistance with the experiments, and also to acknowledge that this work is supported in part by the San Francisco Laser Center, a National Science Foundation Regional Instrumentation Facility, NSF Grant No. CHE-79-16250, operated by the University of California at Berkeley in collaboration with Stanford University.

---

*Permanent address: Department of Physics, University of Alberta, Edmonton, Alberta, Canada T6G 2J1.

[1]L. P. Levine, J. F. Ready, and E. Bernal, J. Appl. Phys. **38**, 331 (1967); IEEE J. Quantum Electron. **QE-4**, 18 (1968).
[2]G. Ertl and M. Neumann, Z. Naturforsch. **27a**, 1607 (1972).
[3]H. Hartwig, P. Mioduszewski, and A. Pospieszczyk, J. Nucl. Mater. **76**, 625 (1978).
[4]J. P. Cowin, D. J. Auerbach, C. Becker, and L. Wharton, Surf. Sci. **78**, 545 (1978).
[5]G. Wedler and H. Ruhmann, Surf. Sci. **121**, 464 (1982).
[6]D. R. Burgess, Jr., R. Viswanathan, I. Hussla, P. C. Stair, and E. Weitz, J. Chem. Phys. **79**, 5200 (1983); D. R. Burgess, Jr., I. Hussla, R. Viswanathan, P. C. Stair, and E. Weitz, Rev. Sci. Instrum. **55**, 1771 (1984).
[7]J. Heidberg, H. Stein, E. Riehl, and A. Nestmann, Z. Phys. Chem. (Neue Folge) **121**, 145 (1980).
[8]J. Heidberg, H. Stein, and E. Riehl, Phys. Rev. Lett. **49**, 666 (1982).
[9]T. J. Chuang and H. Seki, Phys. Rev. Lett. **49**, 382 (1982).
[10]H. Seki and T. J. Chuang, Solid State Commun. **44**, 473 (1982).
[11]T. J. Chuang, J. Electron Spectrosc. Relat. Phenom. **29**, 125 (1983).
[12]T. J. Chuang, Surf. Sci. Rep. **3**, 1 (1983).
[13]Z. W. Gortel, H. J. Kreuzer, P. Piercy, and R. Teshima, Phys. Rev. B **27**, 5066 (1983).
[14]Z. W. Gortel, H. J. Kreuzer, P. Piercy, and R. Teshima, Phys. Rev. B **28**, 2119 (1983).
[15]Z. W. Gortel and H. J. Kreuzer, Phys. Rev. B **29**, 6926 (1984).
[16]T. J. Chuang and I. Hussla, Phys. Rev. Lett. **52**, 2045 (1984).
[17]See, e.g., *Handbook of Chemistry and Physics*, 55th ed. (Chemical Rubber Co., Cleveland, 1974—75), p. E27.
[18]E. Sommer and H. J. Kreuzer, Phys. Rev. B **26**, 4094 (1982).
[19]R. Opila and R. Gomer, Surf. Sci. **112**, 1 (1980).
[20]J. C. Tully, Surf. Sci. **111**, 461 (1981).
[21]D. Lackey, M. Surman, and D. A. King, Vacuum **33**, 867 (1983).
[22]J. L. Gland, B. A. Sexton, and G. E. Mitchell, Surf. Sci. **115**, 623 (1982).
[23]P. S. Bagus, K. Hermann, and C. W. Bauschlicher, Jr., J. Chem. Phys. **81**, 1966 (1984).
[24]D. C. McKean and P. N. Schatz, J. Chem. Phys. **24**, 316 (1956).
[25]P. Pulay and W. Meyer, J. Chem. Phys. **57**, 3337 (1972).
[26]W. M. A. Smit and T. van Dam, J. Chem. Phys. **72**, 3658 (1980).
[27]I. Hussla and T. J. Chuang, Ber. Bunsenges. Phys. Chem. **89**, 294 (1985).